

# Revisiting the Disorder–Order Transition in 1-X-Adamantane Plastic Crystals: Rayleigh Wing, Boson Peak, and Lattice Phonons

Tommaso Salzillo,\* Alberto Girlando, and Aldo Brillante\*

Cite This: *J. Phys. Chem. C* 2021, 125, 7384–7391

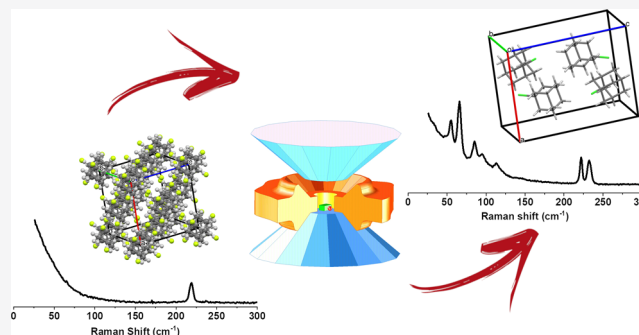
Read Online

ACCESS |

Metrics & More

Article Recommendations

**ABSTRACT:** In this paper, we revisit the disorder–order transition in 1-chloro-adamantane and present new data on 1-bromo-adamantane. Rayleigh scattering and Raman-active optical lattice phonons are used to easily characterize the phase change. Unlike Cl-derivative, the Br-derivative shows a semiordered structure in the vicinity of ambient P,T conditions, which is peculiar of this compound and seems to be due to a more reduced rotational disorder of the Br-derivative with respect to the other halogen-adamantanes. The semiordered phase is briefly discussed in terms of its Rayleigh Wing and Boson peak.



## INTRODUCTION

A disorder–order phase transition is defined as the property of a material to undergo a transition, under pressure, or by lowering the temperature, from a phase where atoms/molecules are arranged randomly with no long-range correlation to a phase in which the system shows a periodic pattern of atoms/molecules with long-range correlation.<sup>1</sup> This phenomenon has been observed on several classes of materials: ionic salts, polymer nanoparticles, metal–organic framework (MOF), perovskite, perovskite–MOF, and liquid crystals.<sup>2–9</sup> These disorder–order phase transitions have gained renewed attention in the past couple of years, in connection with the flourishing research activity on hybrid lead halide perovskites. The reason is due to the flourishing research activity regarding the hybrid lead halide perovskites, a class of materials that are nowadays causing a revolution in photovoltaic research owing to a similar phenomenology.<sup>10–12</sup>

Molecular crystals may show two particular kinds of disorders, the most common being the ability of the molecules or parts of them to switch from one orientation to another within the lattice, while the second one refers to their capability to migrate with relative ease from one site to another.<sup>13</sup> The orientational disorder is also known as a dynamic disorder, or more commonly indicated by the crystallographic community as a thermal disorder, since its magnitude increases by heating up the crystal from low temperature. The effect of the freedom in orientational disorder may be associated with a clear phase transition,<sup>14</sup> even if the molecules start to acquire this freedom well beyond the transition point and the possible orientations are distinguishable. The second type of disorder is usually

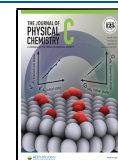
observed only when the molecules in the crystal lattice have gained considerable orientational freedom to diffuse from site to site. In some cases, it is possible to observe the development of both kinds of disorders simultaneously.<sup>15</sup>

A class of crystalline molecular materials that present both types of disorder is represented by plastic crystals. A first attempt to classify these crystals was made in 1961 by J. Timmermans, who analyzed the melting point entropy of several organic and inorganic compounds.<sup>16</sup> More generally, plastic crystals are those crystals that easily undergo plastic deformation. It has been empirically found that in these materials, three peculiar factors can be recognized: (I) the molecules are globular, i.e., possess symmetry around their center or show nearly spherical shapes, (II) the symmetry of the lattice is high, and (III) the barrier to molecular reorientation at a site is relatively low.<sup>17</sup> From the point of view of the symmetry, the plastic crystalline phase displays a long-range translational order but a short-range order with respect to rotation. Like liquid crystals, they can be considered a transitional stage between solid and liquid.<sup>18</sup> The hydrocarbon adamantane (C<sub>10</sub>H<sub>16</sub>) is a typical example of molecules that form plastic crystals. The adamantane molecule consists of three condensed cyclohexane rings connected in a chair conformation, showing an archetypical diamondoid structure

Received: January 11, 2021

Revised: March 12, 2021

Published: March 24, 2021



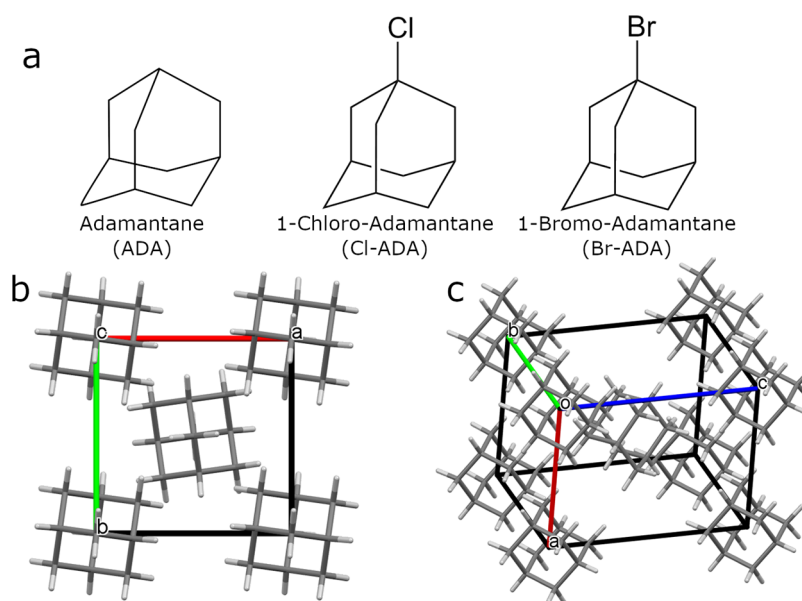


**Figure 1.** (a) Molecular structures of adamantane, 1-chloro-adamantane, and 1-bromo-adamantane. (b) XRD structure of adamantane on the ab-plane (b) and in general orientation (c).

with strong covalent bonds, whereas the intermolecular forces are essentially weak van der Waals forces (Figure 1).

Unsubstituted adamantane presents a phase transition from disorder ( $\alpha$  form) to order ( $\beta$  form) by lowering the temperature (T) or increasing pressure (P), with the ambient conditions being the disordered, plastic crystalline phase.<sup>19</sup> Several X-ray diffraction (XRD) studies<sup>20,21</sup> reported in the literature describe the adamantane phase transition, which shows how the molecules in the ordered phase  $\beta$  are distributed between two mutually perpendicular orientations, whereas in the disordered phase, they are randomly distributed between these two possible orientations. At the same time, by lowering T, the lattice transforms from a cubic disordered phase, which belongs to the centrosymmetric space group  $F43m$  with four molecules per unit cell, into an ordered tetragonal one with the space group  $P4_21c$  and two molecules per unit cell.<sup>20,21</sup> The evident lowering in the symmetry in these disorder-to-order transformations is another peculiar aspect, and it has been reported to be temperature<sup>20–22</sup> or pressure induced.<sup>23</sup> Other techniques have been used for the study of adamantanes such as IR<sup>24</sup> and NMR, the latter having the ability to measure both the relaxation time of the molecular rotational freedom and the very long diffusional jump times.<sup>17,25</sup> Therefore, adamantane and its derivatives represent ideal systems for the study of these disorder–order phase transitions in plastic crystals.

In the present work, we use low-frequency Raman spectroscopy to revisit the pressure-induced phase transition of 1-chloro-adamantane (Cl-ADA) and report new data on the analogous phase transition in 1-bromo-adamantane (Br-ADA). A comparison between these two cases advances the discussion on the nature of the room T,P disordered or semioriented phase, emphasizing the peculiar nature of the Br-derivative with respect to the other 1-halogen-adamantanes.

The study under pressure by low-frequency Raman spectroscopy is strategic, in that the intermolecular modes occurring in this region, called optical lattice phonons, are the ideal probe to monitor the molecular environment in the unit

cell, well complementing the structural data provided by the XRD experiments.

## EXPERIMENTAL SECTION

Cl-ADA and Br-ADA were purchased both from Sigma-Aldrich with a purity of 98 and 99%, respectively, and used for the spectroscopic measurements without further purification.

Low-frequency micro-Raman spectra were obtained with a Jobin Yvon T64000 triple grating Raman spectrometer, in double subtractive mode, interfaced with an optical microscope (Olympus BX40) with 50 $\times$  or 100 $\times$  objectives. Working in confocality allowed us to obtain a spatial resolution below 0.9  $\mu\text{m}$ . Spectra were recorded spanning the low-wavenumber region of the lattice phonons (10–150  $\text{cm}^{-1}$ ) up to about 400  $\text{cm}^{-1}$  to detect the lower-wavenumber intramolecular vibrations for both Cl-ADA and Br-ADA. The excitation was from a krypton laser tuned at 647.1 nm, excitation energy sufficiently low to avoid the background photoluminescence. The incoming power was reduced with a series of neutral density filters to prevent crystal damage, with the actual power focused on the sample being anyway less than 1 mW.

High-pressure measurements were performed in a diamond anvil cell (DAC) with an in-house design with stainless steel gasket of 0.3 mm diameter. A 4:1 methanol–ethanol mixture was used as a hydrostatic medium, and pressures were calibrated with the standard ruby luminescence method.<sup>26,27</sup>

## RESULTS AND DISCUSSION

**1-Chloro-adamantane.** Cl-ADA ( $\text{C}_{10}\text{H}_{15}\text{Cl}$ ) is a well-known adamantane derivative obtained by replacing one hydrogen bound to a tertiary carbon atom with chlorine (Figure 1). The substitution of the hydrogen atom with chlorine lowers the tetrahedral ( $T_d$ ) molecular symmetry of the parent molecule to  $C_{3v}$ .<sup>28</sup> At room temperature and atmospheric pressure, Cl-ADA, like other adamantane derivatives, resides in a state of orientationally disordered plastic phase defined as phase I. Foulon et al. refined the high-temperature disordered phase as a face-centered cubic (fcc) lattice with a space group  $Fm\bar{3}m$ , with four molecules per unit

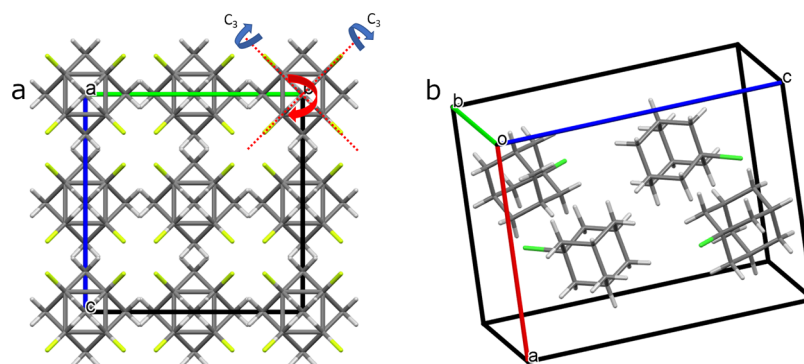


**Figure 2.** Projections of the high-temperature plastic phase structure in the  $bc$ -plane showing the molecules at the center of mass of the cubic lattice with arbitrary random local arrangements (a). Structure of the low-temperature ordered monoclinic phase (b).

cell. The ordered low-temperature phase III belongs to a monoclinic system, space group  $P2_1/c$ , and four molecules per unit cell (Figure 2).<sup>28</sup>

The dynamic molecular disorder characteristic of phase I has been probed in an elegant study by NMR and incoherent quasi-elastic neutron scattering, showing that the motions responsible for this disorder are a combined effect of uniaxial rotations of both the molecule and the crystal, as well as molecular diffusion like the parent adamantane.<sup>19,29</sup> The sum of uniaxial rotations around the molecular threefold axis  $C_3$  (blue arrows in Figure 2) and around the cell axis (red arrow in Figure 2) generate 12 different configurations ( $M_{12}$ ) of the molecule at the center of mass, as represented in Figure 2.

Similarly to the parent adamantane, Cl-ADA undergoes a disorder–order phase transition by lowering the temperature (246 K) or by applying pressure (0.5 GPa).<sup>30,31</sup>

Additionally, a non-first-order phase transition takes place at around 320 K, without a change in the lattice symmetry, as revealed by an anomaly hump in the observed calorimetric measurement.<sup>32</sup> This is explained by the existence of a purely orientational disorder–disorder phase transition, without a noticeable change in the molecular positions, i.e., a change purely driven by the reorientational dynamics that occurs slightly above room temperature.

For this compound, we first revisit the Raman scattering spectrum, limiting the attention to the low-frequency modes, with special emphasis to the lattice phonons, which represent the ideal tool to probe the symmetry environment of the unit cell.<sup>33–36</sup> Then, new data on Br-ADA allow us to make a comparison between these two halogen-adamantanes.

Figure 3 shows the pressure dependence of the Raman-active lattice phonons and the low-intramolecular modes below  $400\text{ cm}^{-1}$  of the chloroderivative. The spectral profiles agree well with the detailed data reported by Hédoux et al.,<sup>30</sup> obtained in a DAC without hydrostatic conditions. The most spectacular result is the sudden appearance of the phonon structure at 1 GPa, just above the pressure-induced phase transition at 0.5 GPa. The structured phonon spectrum on increasing pressure is the clear indication of a crystalline fully ordered phase. Below the transition pressure, the phonon pattern is washed away, a consequence of the impossibility of a phase matching in a disordered, nonperiodical structure. The equivalent in XRD is the broadening of the diffraction peaks in a disordered phase, eventually leading to a flat background at the complete amorphization.

The diffuse Rayleigh wing (RW) starting around  $80\text{ cm}^{-1}$  is instead due to the elastic scattering centered at  $\omega = 0$ , the

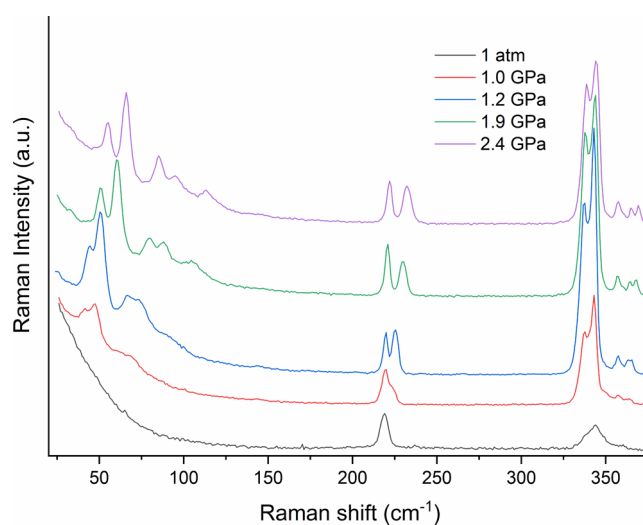


**Figure 3.** Raman spectra of 1-chloro-adamantane at several pressures in the selected spectral region.

frequency of the exciting laser. This effect is more common in inorganic materials where it is defined as “central peak” and is the consequence of distortion motions induced by impurities in the unit cell, which either break the symmetry<sup>37</sup> or undergo a second-order structural phase transition.<sup>38</sup> A wide RW is also a characteristic feature of spectra of light scattered in liquids and its spectral form is strongly influenced by the chemical composition and the temperature of the liquid itself.<sup>39</sup> Accordingly, the increased RW below 0.5 GPa is here attributed to the orientational molecular motions paradigmatic of a disordered system, and its intensity follows the statistical distribution of reorientation times as the full width at half-maximum (FWHM) sharpens by increasing temperature<sup>31</sup> or decreasing pressure. This effect is common to highly viscous liquids and is a typical feature in the Raman spectrum of molecular crystals at melting.<sup>40</sup>

Useful information can also be drawn by looking at the wavenumber region of the lowest intramolecular modes. At ambient conditions, the first intramolecular intensity band is the C–Cl bending at about  $220\text{ cm}^{-1}$ . Its symmetry is diagnostic of the disorder–order phase transition because although it is a single degenerate band of  $E_g$  symmetry at low pressure,<sup>30</sup> it splits into a doublet  $A_g + B_g$  on increasing the pressure because the symmetry is reduced in the monoclinic ordered phase, space group  $P2_1/c$  with four molecules per unit cell.<sup>28</sup>

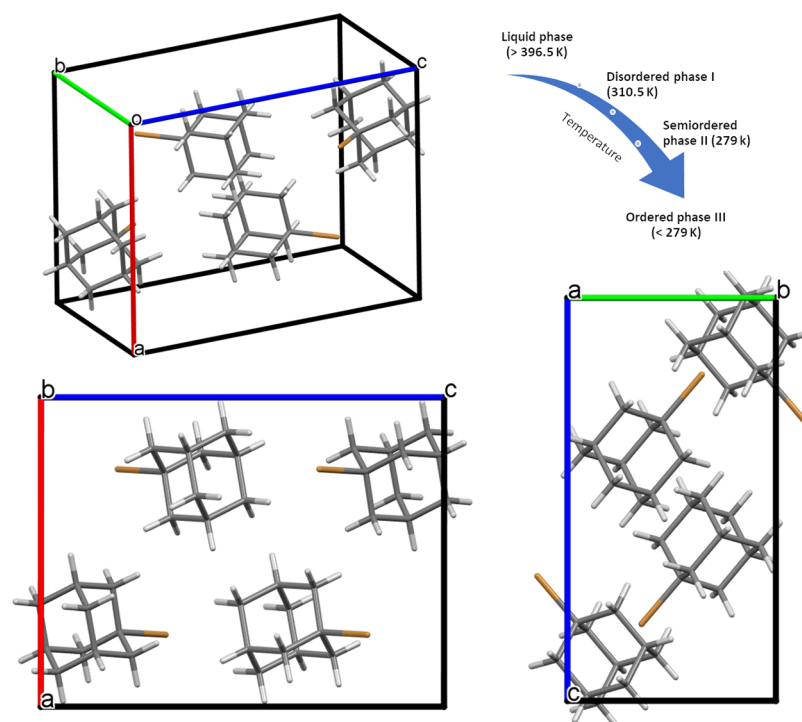


Figure 4. Structure of the ordered phase III of 1-bromo-adamantane.

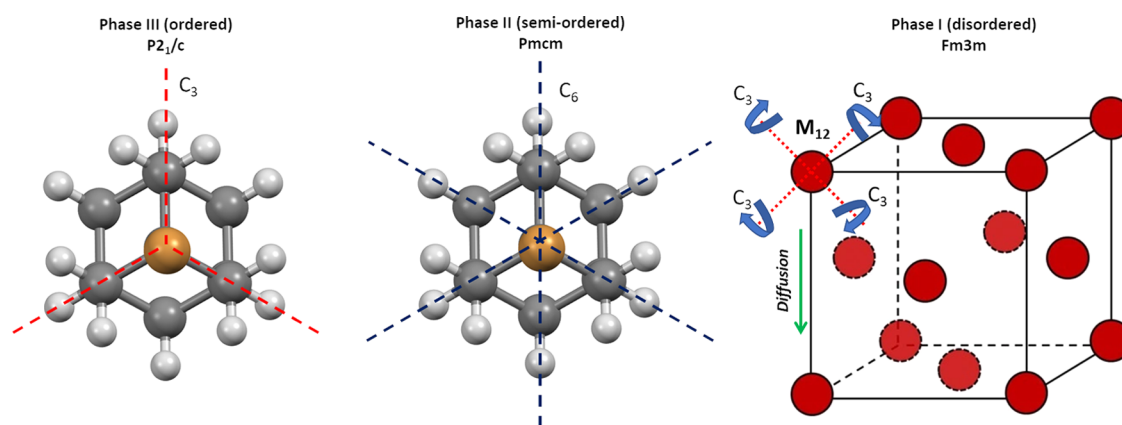


Figure 5. Characteristic motions in the three phases of 1-bromo-adamantane.

The residual RW above 0.5 GPa can be explained by assuming that even above the transition pressure, the disorder–order change is not complete. In other words, we assume that the reorientational disorder typical of the ambient pressure phase, although considerably decreased, keeps still a not negligible component at the higher pressures. This assumption is in agreement with the quasi-elastic neutron scattering study by Bée et al.,<sup>29</sup> who hypothesized the presence of a residual reorientational disorder after the temperature-induced transition (246 K).

**1-Bromo-adamantane.** Likewise, the other disordered phases of adamantane derivatives, the phase I of Br-ADA ( $C_{10}H_{15}Br$ ), exhibit the fcc lattice and space group  $Fm3m$  with four molecules per unit cell. The exact coordinates of the atomic positions are unknown due to the highly dynamic disorder characteristic of the plastic crystals in the disordered phase.

The structure of the ordered phase III of Br-ADA has only recently been solved. At low  $T$  (below 279 K) or high  $P$  (>0.5

GPa), Br-ADA crystallizes in a monoclinic system, space group  $P2_1c$  with four molecules per unit cell (Figure 4).<sup>41</sup>

Among the 1-adamantyl halides, Br-ADA represents an exception regarding the crystal ordering with respect to the temperature and pressure gradients. Indeed, while the other 1-adamantyl halides so far investigated show a phase I to phase III disorder–order transition, Br-ADA has an intermediate semiordered phase II between 279 and 310.5 K.<sup>42</sup> Clark et al.<sup>43</sup> proposed a mechanism of transition from phase I to phase III via a formation of an intermediate semiordered phase on the basis of the values of the transition entropies. The XRD investigation confirms the existence of this semiordered phase<sup>44</sup> as orthorhombic, space group  $Pmcn$  with four molecules per unit cell, showing orientational disorder but with different degrees of freedom compared to phases I and III.

With the combination of NMR and XRD temperature dependence studies, the molecular motions responsible for the disorder have been proposed. In phase I, the overall molecular tumbling and the slower diffusion process are dominating,



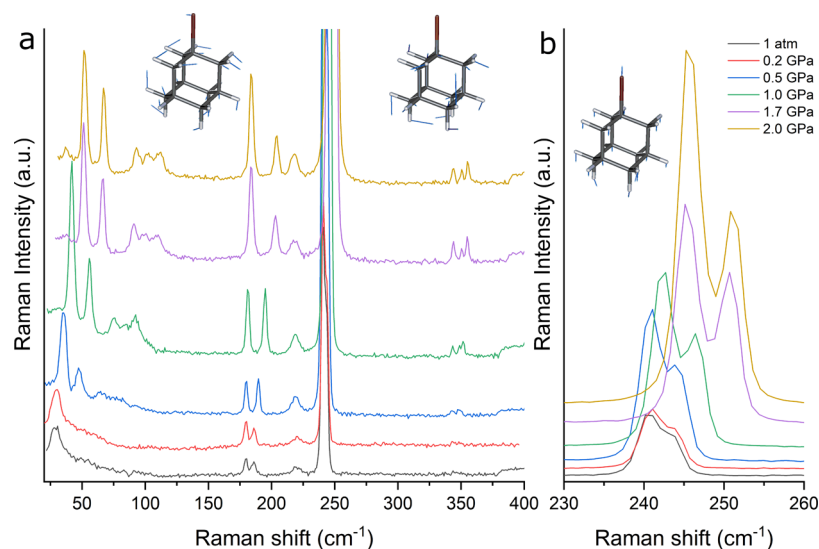


**Figure 6.** (a) Raman spectra of 1-bromo-adamantane at several pressures in the 20–400  $\text{cm}^{-1}$  spectral region. (b) An enlarged view of the C–Br stretching region.

whereas, with the increased order, the motions are limited to reorientations about the sixfold axis for phase II and rotations about the  $C_3$  molecular axis in phase III, with two crystallographically discernible positions (Figure 5).<sup>42,45</sup>

At high pressure, a Fourier transform infrared (FT-IR) spectroscopy study<sup>46</sup> reports the phase transition from a semiorde to order occurring at 0.5 GPa using changes in the intensity ratio of specific vibrational modes.

In Figure 6, we show the pressure dependence of Raman spectra, analyzing both the lattice dynamics in the low-frequency range and the molecular dynamics in the higher-wavenumber region.

To better assign the lowest intramolecular modes of Br-ADA, we have calculated the vibrational frequencies and the Raman normal modes starting by searching the equilibrium geometry of the isolated molecule with an ab initio program. We have used GAMESS 2019 R1,<sup>47</sup> with the B3LYP/6-31G(d) combination of exchange-correlation functional and basis set, and the outputs were analyzed by Gabedit.<sup>48</sup> In the range 150–400  $\text{cm}^{-1}$ , a number of bands have been identified. The two peaks below 200  $\text{cm}^{-1}$  at ambient pressure are the bending modes of the C–Br bond and computed as two distinct vibrations in the isolated molecule. Their split is interpreted in the same way as its analogous chloroderivative, i.e., as the symmetry lowering from a cubic to a monoclinic group. They appear at lower wavenumbers with respect to Cl-ADA, as expected by the increased reduced mass. The very intense peak centered at about 236  $\text{cm}^{-1}$  is the C–Br stretching, which is computed as single mode in the isolated molecule. In the experimental spectrum, even at ambient pressure, it clearly appears as an asymmetric band that, by increasing pressure, ends up into two distinct bands. This doublet also recalls the  $A_g + B_g$  splitting observed in Cl-ADA under pressure, and this confirms that the crystal symmetry of Br-ADA below the transition pressure of 0.5 GPa is different from the completely disordered structure that belongs to the cubic phase I. Since Br-ADA shows the first disorder (phase I) to semiorde (phase II) transition at 310 K, we believe that the spectrum at ambient pressure already refers to the semiorde phase II. Finally, at about 350  $\text{cm}^{-1}$ , three peaks are identified

and computed as characteristic breathing modes of the diamondoid structure.

The corresponding eigenvectors calculated for the most intense normal modes in the 150–400  $\text{cm}^{-1}$  range are reported as insets in Figure 6.

This result is convincingly confirmed by looking at the low-frequency range, which is characterized, contrary to the case of Cl-ADA, by two specific features at ambient pressure: (1) it presents a smaller RW component, as a result of the effect of the dynamic disorder, and (2) it shows the presence of a broadband centered at around 30  $\text{cm}^{-1}$ .

As to the first point, the reduced width of the RW indicates that we are indeed above the transition pressure of the disordered phase I. However, the lack of the entire phonon spectrum clearly shows that this state is not fully ordered. We can quite plausibly assume that we are in the presence of the semiorde phase II, as indicated by the intramolecular vibrations detailed above.

As to the second point, we privilege the interpretation that this spectral feature is reminiscent of the shape of the Boson peak observed in the Raman spectra of inorganic heterogeneous structures or in molecular glass-forming materials.<sup>49,50</sup> Although this definition is still a subject of debate, it is undoubtedly associated with an intermediate-range order,<sup>51</sup> as due to a residual molecular correlation in glass or semiorde materials. In the present case, it can be considered as the Raman signature of dynamic relaxation of the semiorde phase II of Br-ADA. Indeed, some hints can be drawn by relating this broad feature at 0.2 GPa to the full phonon spectrum of the ordered phase (III) at higher pressure. The band of this semiorde phase is, in fact, broad and peaked at about 28  $\text{cm}^{-1}$ . Taking into account a reasonable pressure shift and a drastic reduction of its inhomogeneous broadening, this band can well be correlated to the lowest-wavenumber phonon of the ordered phase, evolving to about 36  $\text{cm}^{-1}$  at 0.5 GPa and 42  $\text{cm}^{-1}$  at 1.0 GPa.

With this in mind, if we analyze the nature of the six Raman-active lattice phonons of Br-ADA, we easily end up with their symmetry assignment as  $(3A_g + 3B_g)$ . In the presence of a center of symmetry, as in the  $P2_1c$  space group, all six modes are librational in nature, and due to the collective partial

rotations (g-symmetry) of the molecules, around their inertia axes, in the unit cell. The expected pattern of decreasing frequency for increasing the moment of inertia suggests that the lowest-wavenumber phonon corresponds to the largest inertia moment, which is the rotation around the threefold rotational axis of the molecules ( $C_3$ ). One can then argue that the so-called Boson peak is none other than the collective rotational of the  $2\pi/6$  degree of freedom of the semioordered phase that, with increasing pressure, leads to a tilting of the molecular axes up to reach their full alignment in the perfectly ordered structure of the monoclinic phase. A sketch of this transition is schematically shown in Figure 5.

The transition at 0.5 GPa from phase II to III, like Cl-ADA, still shows a residual RW component till 1.0 GPa. In fact, the system can still possess the threefold reorientational degree of freedom characteristic of the ordered phase of the other halogen-adamantanes ( $X = F, Cl$ ). By further increasing pressure, the RW disappears completely and this effect can be attributed to the complete freezing of the reorientational disorder at very high pressure. A numerical experiment by Ashcroft et al. has rationalized this finding by analyzing the pressure dependence of the rotational energy around the molecular  $C_6$  axis of benzene in its phase III.<sup>52</sup>

## CONCLUSIONS

Br-ADA represents a peculiar case in the system of the halogen-adamantanes. In fact, fluoro-<sup>53</sup> and chloro-substituted adamantanes both present a disorder–order phase transition from phase I to phase III, without showing the transition to the semioordered intermediate phase. I-Iodo-adamantane (I-ADA) does not show a plastic disordered phase III but only a semioordered phase II, in the range 211–347 K, before melting and the ordered phase III, below 211 K.<sup>54</sup> This is in agreement with the first observation by Timmermans, who established the melting entropy limit of 5 e.u. (about  $21 \text{ J K}^{-1} \text{ mol}^{-1}$ ) for plastic crystals.<sup>16</sup> Cl-ADA and Br-ADA have 11.01 and  $9.74 \text{ J K}^{-1} \text{ mol}^{-1}$ , respectively, of melting entropy, whereas I-ADA has a higher melting entropy value of  $29.45 \text{ J K}^{-1} \text{ mol}^{-1}$ , which overcomes the limit for the plastic crystals.<sup>43</sup> Nevertheless, both Br-ADA and I-ADA show a semioordered phase where the tumbling reorientational rotations ( $M_{12}$ ) are not present, as opposed to that observed for the other halogen-adamantanes. The absence of this disorder can be attributed to the different bond lengths of the C–X, which increases in the Br-ADA and I-ADA, influencing the moment of inertia.<sup>55</sup> The increased moment of inertia requires more energy for the tumbling disorder and this partially reduces the motions in Br-ADA below 310 K and completely hinders I-ADA, whose the only reorientation is allowed along the principal molecular axis.

As pointed above, Br-ADA is the only adamantane showing plastic to semioordered structure transition in the vicinity of ambient P,T conditions, and this peculiar behavior is due to a more reduced rotational disorder of the Br-derivative with respect to the other halogen-adamantanes.

Whereas the elastic scattering yields a prompt diagnosis of the degree and the dynamics of orientational disorder of the system, as observed by the width of the RW, the anelastic scattering manifests the dynamics of the intermolecular modes. A distinct lattice phonon spectrum is a clear indication of a state of order derived by the periodicity of the crystal lattice in response to the incoming e.m. field. As long as the degree of disorder starts to appear, the structured phonon spectrum is washed away as a consequence of the lack of phase matching of

the momentum of incoming photon and scattered phonon. The presence in Br-ADA of the intermediate semioordered phase between the fully ordered and the fully disordered structures is very clearly signaled by the appearance of a distinctive, unique Raman band around  $27 \text{ cm}^{-1}$ , reminiscent of what is sometimes described as the Boson peak. This feature, although revealing the absence of a crystal lattice, is nevertheless the indication of an intermediate-range correlation in quasi-isotropic systems.

The synergy between Rayleigh scattering and Raman phonon spectroscopy has been successfully used to obtain a detailed characterization of Cl-ADA and Br-ADA phase changes under pressure. Pressure acts, in fact, as a powerful solvent effect, with strong consequences on the dispersion forces that are exemplarily probed by intermolecular vibrations, such as lattice phonons, the more so for soft materials.

## AUTHOR INFORMATION

### Corresponding Authors

Tommaso Salzillo – Department of Chemical and Biological Physics, Weizmann Institute of Science, 76100 Rehovot, Israel; [orcid.org/0000-0002-9737-2809](https://orcid.org/0000-0002-9737-2809);

Email: [tommaso.salzillo@unibo.it](mailto:tommaso.salzillo@unibo.it)

Aldo Brillante – Dipartimento di Chimica Industriale “Toso Montanari”, Università di Bologna, Bologna 40136, Italy; Email: [aldo.brillante@unibo.it](mailto:aldo.brillante@unibo.it)

### Author

Alberto Girlando – Molecular Materials Group, 43124 Parma, Italy; [orcid.org/0000-0003-1887-709X](https://orcid.org/0000-0003-1887-709X)

Complete contact information is available at: <https://pubs.acs.org/10.1021/acs.jpcc.1c00239>

### Notes

The authors declare no competing financial interest.

## ACKNOWLEDGMENTS

T.S. thanks Dr. Omer Yaffe for useful discussions.

## REFERENCES

- (1) Cairns, A. B.; Goodwin, A. L. Structural Disorder in Molecular Framework Materials. *Chem. Soc. Rev.* **2013**, *42*, 4881–4893.
- (2) Collings, I. E.; Bykov, M.; Bykova, E.; Hanfland, M.; Van Smaalen, S.; Dubrovinsky, L.; Dubrovinskaia, N. Disorder-Order Transitions in the Perovskite Metal-Organic Frameworks [(CH<sub>3</sub>)<sub>2</sub>NH<sub>2</sub>][M(HCOO)<sub>3</sub>] at High Pressure. *CrystEngComm* **2018**, *20*, 3512–3521.
- (3) Bellin, C.; Mafety, A.; Narayana, C.; Giura, P.; Rouse, G.; Itié, J. P.; Polian, A.; Saitta, A. M.; Shukla, A. Disorder-Order Phase Transition at High Pressure in Ammonium Fluoride. *Phys. Rev. B* **2017**, *96*, No. 094110.
- (4) Park, B. W.; Philippe, B.; Gustafsson, T.; Sveinbjörnsson, K.; Hagfeldt, A.; Johansson, E. M. J.; Boschloo, G. Enhanced Crystallinity in Organic-Inorganic Lead Halide Perovskites on Mesoporous TiO<sub>2</sub> via Disorder-Order Phase Transition. *Chem. Mater.* **2014**, *26*, 4466–4471.
- (5) Higuchi, T.; Motoyoshi, K.; Sugimori, H.; Jinnai, H.; Yabu, H.; Shimomura, M. Phase Transition and Phase Transformation in Block Copolymer Nanoparticles. *Macromol. Rapid Commun.* **2010**, *31*, 1773–1778.
- (6) Xu, G. C.; Ma, X. M.; Zhang, L.; Wang, Z. M.; Gao, S. Disorder-Order Ferroelectric Transition in the Metal Formate Framework of [NH<sub>4</sub>][Zn(HCOO)<sub>3</sub>]. *J. Am. Chem. Soc.* **2010**, *132*, 9588–9590.

- (7) Dolganov, V. K.; Gal, M.; Kroo, N.; Rosta, L.; Sheka, E. F. Evolution of the Coherence of Vibrational States in a Gradual Disorder-Order Phase Transition. *J. Mol. Struct.* **1984**, *114*, 325–328.
- (8) Postorino, P.; Malavasi, L. Pressure-Induced Effects in Organic-Inorganic Hybrid Perovskites. *J. Phys. Chem. Lett.* **2017**, *8*, 2613–2622.
- (9) Sharma, R.; Menahem, M.; Dai, Z.; Gao, L.; Brenner, T. M.; Yadgarov, L.; Zhang, J.; Rakita, Y.; Korobko, R.; Pinkas, I.; et al. Halide Perovskites under Polarized Light: Vibrational Symmetry Analysis Using Polarized Raman. *Phys. Rev. Materials* **2019**, *4*, No. 51601.
- (10) Bakulin, A. A.; Selig, O.; Bakker, H. J.; Rezus, Y. L. A.; Müller, C.; Glaser, T.; Lovrincic, R.; Sun, Z.; Chen, Z.; Walsh, A.; et al. Real-Time Observation of Organic Cation Reorientation in Methylammonium Lead Iodide Perovskites. *J. Phys. Chem. Lett.* **2015**, *6*, 3663–3669.
- (11) Francisco-López, A.; Charles, B.; Weber, O. J.; Alonso, M. I.; Garriga, M.; Campoy-Quiles, M.; Weller, M. T.; Goñi, A. R. Pressure-Induced Locking of Methylammonium Cations versus Amorphization in Hybrid Lead Iodide Perovskites. *J. Phys. Chem. C* **2018**, *122*, 22073–22082.
- (12) Leguy, A. M. A.; Goñi, A. R.; Frost, J. M.; Skelton, J.; Brivio, F.; Rodríguez-Martínez, X.; Weber, O. J.; Pallipurath, A.; Alonso, M. I.; Campoy-Quiles, M.; et al. Dynamic Disorder, Phonon Lifetimes, and the Assignment of Modes to the Vibrational Spectra of Methylammonium Lead Halide Perovskites. *Phys. Chem. Chem. Phys.* **2016**, *18*, 27051–27066.
- (13) Parsonage, N. G.; Staveley, L. A. K. *Disorder in Crystals*; Oxford University Press/Clarendon Oxford: Oxford, 1978.
- (14) Chung, H.; Dudenko, D.; Zhang, F.; D'Avino, G.; Ruzié, C.; Richard, A.; Schweicher, G.; Cornil, J.; Beljonne, D.; Geerts, Y.; et al. Rotator Side Chains Trigger Cooperative Transition for Shape and Function Memory Effect in Organic Semiconductors. *Nat. Commun.* **2018**, *9*, No. 278.
- (15) Sherwood, J. N. *The Plastically Crystalline State*; John Wiley & Sons Limited: Chichester, New York, Brisbane, Toronto, 1979.
- (16) Timmermans, J. Plastic Crystals: A Historical Review. *J. Phys. Chem. Solids* **1961**, *18*, 1–8.
- (17) Resing, H. A. NMR Relaxation in Adamantane and Hexamethylenetetramine: Diffusion and Rotation. *Mol. Cryst. Liq. Cryst.* **1969**, *9*, 101–132.
- (18) Das, S.; Mondal, A.; Reddy, C. M. Harnessing Molecular Rotations in Plastic Crystals: A Holistic View for Crystal Engineering of Adaptive Soft Materials. *Chem. Soc. Rev.* **2020**, *49*, 8878–8896.
- (19) Fyfe, C. A.; Harold-Smith, D. Potential Energy Calculations of the Mechanisms of Self-Diffusion in Molecular Crystals: Adamantane. *Can. J. Chem.* **1976**, *54*, 783–789.
- (20) Nordman, C. E.; Schmitkons, D. L. Phase Transition and Crystal Structures of Adamantane. *Acta Crystallogr.* **1965**, *18*, 764–767.
- (21) Amoureux, J. P.; Foulon, M. Comparison Between Structural Analyses of Plastic and Brittle Crystals. *Acta Crystallogr., Sect. B: Struct. Sci., Cryst. Eng. Mater.* **1987**, *B43*, 470–479.
- (22) Gromnitskaya, E. L.; Danilov, I. V.; Brazhin, V. V. Comparative Study of the Elastic Properties of Adamantane and 1-Chloroadamantane at High Pressure and Different Temperatures and at Order-Disorder Transitions. *Phys. Chem. Chem. Phys.* **2021**, *23*, 2349–2354.
- (23) Ito, T. Pressure-Induced Phase Transition in Adamantanone. *Acta Crystallogr., Sect. B: Struct. Sci., Cryst. Eng. Mater.* **1973**, *29*, 364–365.
- (24) Wu, P.-J.; Hsu, L.; Dows, D. A. Spectroscopic Study of the Phase Transition in Crystalline Adamantane. *J. Chem. Phys.* **1971**, *54*, 2714–2721.
- (25) Resing, H. A. Confirmation of Phase Change in Solid Adamantane by NMR. *J. Chem. Phys.* **1965**, *43*, 1828–1829.
- (26) Shen, G.; Wang, Y.; Dewaele, A.; Wu, C.; Fratanduono, D. E.; Eggert, J.; Klotz, S.; Dziubek, K. F.; Loubeyre, P.; Fat'yanov, O. V.; Asimov, P. D.; et al. Toward an International Practical Pressure Scale: A Proposal for an IPPS Ruby Gauge (IPPS-Ruby2020). *High Pressure Res.* **2020**, *40*, 299–314.
- (27) Piermarini, G. J.; Block, S.; Barnett, J. D.; Forman, R. A. Calibration of the Pressure Dependence of the R1 Ruby Fluorescence Line to 195 Kbar. *J. Appl. Phys.* **1975**, *46*, 2774–2780.
- (28) Foulon, M.; Belgrand, T.; Gors, C.; More, M. Structural Phase Transition in 1-chloroadamantane (C10H15Cl). *Acta Crystallogr., Sect. B: Struct. Sci., Cryst. Eng. Mater.* **1989**, *45*, 404–411.
- (29) Bée, M.; Amoureux, J. P. Molecular Reorientations of 1-Chloroadamantane in Its Plastic Solid Phase. *Mol. Phys.* **1983**, *48*, 63–79.
- (30) Hédoux, A.; Guinet, Y.; Capet, F.; Affouard, F.; Descamps, M. Raman Effects under Pressure in Chloroadamantane Plastic Crystal. *J. Phys.: Condens. Matter* **2002**, *14*, 8725–8741.
- (31) Affouard, F.; Guinet, Y.; Denicourt, T.; Descamps, M. Indication for a Change of Dynamics in Plastic Crystal Chloroadamantane: Raman Scattering Experiment and Molecular Dynamics Simulation. *J. Phys.: Condens. Matter* **2001**, *13*, 7237–7248.
- (32) Vispa, A.; Monserrat, D.; Cuello, G. J.; Fernandez-Alonso, F.; Mukhopadhyay, S.; Demmel, F.; Tamarit, J. L.; Pardo, L. C. On the Microscopic Mechanism behind the Purely Orientational Disorder-Disorder Transition in the Plastic Phase of 1-Chloroadamantane. *Phys. Chem. Chem. Phys.* **2017**, *19*, 20259–20266.
- (33) Soccia, J.; Salzillo, T.; Della Valle, R. G.; Venuti, E.; Brillante, A. Fast Identification of Rubrene Polymorphs by Lattice Phonon Raman Microscopy. *Solid State Sci.* **2017**, *71*, 146–151.
- (34) Salzillo, T.; Giunchi, A.; Masino, M.; Bedoya-Martínez, N.; Della Valle, R. G.; Brillante, A.; Girlando, A.; Venuti, E. An Alternative Strategy to Polymorph Recognition at Work: The Emblematic Case of Coronene. *Cryst. Growth Des.* **2018**, *18*, 4869–4873.
- (35) Salzillo, T.; Rivalta, A.; Castagnetti, N.; D'Agostino, S.; Masino, M.; Grepioni, F.; Venuti, E.; Brillante, A.; Girlando, A. Spectroscopic Identification of Quinacridone Polymorphs for Organic Electronics. *CrystEngComm* **2019**, *21*, 3702–3708.
- (36) Brillante, A.; Bilotti, I.; Della Valle, R. G.; Venuti, E.; Girlando, A. Probing Polymorphs of Organic Semiconductors by Lattice Phonon Raman Microscopy. *CrystEngComm* **2008**, *10*, 937–946.
- (37) Halperin, B. I.; Varma, C. M. Defects and the Central Peak near Structural Phase Transitions. *Phys. Rev. B* **1976**, *14*, 4030–4044.
- (38) Vugmeister, B. E.; Yacoby, Y.; Toulouse, J.; Rabitz, H. Second-Order Central Peak in the Raman Spectra of Disordered Ferroelectrics. *Phys. Rev. B: Condens. Matter Mater. Phys.* **1999**, *59*, 8602–8606.
- (39) Malinovsky, V. K.; Novikov, V. N.; Sokolov, A. P. Evolution of the Rayleigh Line Wing and Structural Correlations for Liquid-Glass Transition. *Phys. Lett. A* **1987**, *123*, 19–22.
- (40) Fabelinskii, I. *Molecular Scattering of Light*, Springer-Verlag, Ed.; Springer: Boston, MA, 1968.
- (41) Betz, R.; Klüfers, P.; Mayer, P. 1-Bromo-Adamantane. *Acta Crystallogr., Sect. E: Struct. Rep. Online* **2009**, *E65*, No. o101.
- (42) Bazyleva, A. B.; Blokhin, A. V.; Kabo, G. J.; Kabo, A. G.; Paulechka, Y. U. Thermodynamic Properties of 1-Bromoadamantane in the Condensed State and Molecular Disorder in Its Crystals. *J. Chem. Thermodyn.* **2005**, *37*, 643–657.
- (43) Clark, T.; Knox, T. M. O.; Mackle, H.; McKervey, M. A. Order-Disorder Transitions in Substituted Adamantanes. *J. Chem. Soc., Faraday Trans. 1* **1977**, *73*, 1224–1231.
- (44) Zieliński, P.; Foulon, M. In *Dynamics of Molecular Crystals*; Lascombe, J., Ed.; Elsevier: Amsterdam, 1987.
- (45) Huang, Y.; Gilson, D. F. R.; Butler, I. S.; Morin, F. Study of Molecular Motions in the Orientationally Disordered Organic Solids 1-Bromoadamantane and 1-Adamantanecarboxylic Acid by <sup>13</sup>C NMR Spin-Lattice Relaxation and Dipolar Decoupling Time Measurements. *J. Phys. Chem. A* **1991**, *95*, 2151–2156.
- (46) Fraczyk, L. A.; Huang, Y. A High Pressure FT-IR Spectroscopic Study of Phase Transitions in 1-Chloro- and 1-Bromoadamantane. *Spectrochim. Acta, Part A* **2001**, *57*, 1061–1071.
- (47) Barca, G. M. J.; Bertoni, C.; Carrington, L.; Datta, D.; De Silva, N.; Deustua, J. E.; Fedorov, D. G.; Gour, J. R.; Gunina, A. O.; Guidez,

E.; et al. Recent Developments in the General Atomic and Molecular Electronic Structure System. *J. Chem. Phys.* **2020**, *152*, No. 154102.

(48) Allouche, A. Software News and Updates Gabedit - A Graphical User Interface for Computational Chemistry Softwares. *J. Comput. Chem.* **2011**, *32*, 174–182.

(49) Malinovsky, V. K.; Novikov, V. N.; Sokolov, A. P. Log-Normal Spectrum of Low-Energy Vibrational Excitations in Glasses. *Phys. Lett. A* **1991**, *153*, 63–66.

(50) Alba-Simionesco, C.; Krakoviak, V.; Krauzman, M.; Migliardo, P.; Romain, F. Low-Wavenumber Raman Scattering of Molecular Glass-Forming Liquids. *J. Raman Spectrosc.* **1996**, *27*, 715–721.

(51) Ando, M. F.; Benzine, O.; Pan, Z.; Garden, J. L.; Wondraczek, K.; Grimm, S.; Schuster, K.; Wondraczek, L. Boson Peak, Heterogeneity and Intermediate-Range Order in Binary SiO<sub>2</sub>-Al<sub>2</sub>O<sub>3</sub> Glasses. *Sci. Rep.* **2018**, *8*, No. 5394.

(52) Wen, X. D.; Hoffmann, R.; Ashcroft, N. W. Benzene under High Pressure: A Story of Molecular Crystals Transforming to Saturated Networks, with a Possible Intermediate Metallic Phase. *J. Am. Chem. Soc.* **2011**, *133*, 9023–9035.

(53) Ben Hassine, B.; Negrier, P.; Romanini, M.; Barrio, M.; Macovez, R.; Kallel, A.; Mondieig, D.; Tamarit, J. L. Structure and Reorientational Dynamics of 1-F-Adamantane. *Phys. Chem. Chem. Phys.* **2016**, *18*, 10924–10930.

(54) Foulon, M.; Gors, C. Structure and Steric Hindrance Analyses to Determine the Dynamical Disorder in 1-iodoadamantane (C<sub>10</sub>H<sub>15</sub>I). *Acta Crystallogr., Sect. B: Struct. Sci., Cryst. Eng. Mater.* **1988**, *44*, 156–163.

(55) Chadwick, D.; Legon, A. C.; Millen, D. J. Microwave Spectra and Structures of 1-Cyano- and 1-Iodo-Adamantane. *J. Chem. Soc., Faraday Trans. 2* **1972**, *68*, 2064–2069.